

# Supporting Information

Tomasi et al. 10.1073/pnas.1303346110

## SI Methods

**Subjects.** Inclusion criteria were as follows: (i) ability to understand and give informed consent, and (ii) 18–55 y of age. Exclusion criteria were as follows: (iii) present or past history of neurological, psychiatric, or substance abuse disorder (other than nicotine); (iv) use of psychoactive medications in the past month; (v) current use of prescription medications; (vi) medical conditions that may alter brain function; (vii) cardiovascular disease and diabetes; (viii) history of head trauma with loss of consciousness of more than 30 min; (ix) history of claustrophobia; and (x) contraindications to MRI environment (metallic implants/claustrophobia).

**MRI Acquisition.** The participants were instructed to remain silent, motionless, and awake with their eyes open during the 5-min resting-state scan. Earplugs (28-dB sound pressure level attenuation; 3M Company), headphones (30-dB sound pressure level attenuation; Resonance Technology), and a “quiet” acquisition approach were used to minimize the interference effect of scanner noise during resting-state functional magnetic resonance imaging (R-fMRI) (1). Anatomical images were collected using a T1-weighted 3D-modified driven equilibrium Fourier transform sequence (2) [echo time (TE)/repetition time (TR), 7/15 ms;  $0.94 \times 0.94 \times 1$  mm spatial resolution; axial orientation; 256 readout and  $192 \times 96$  phase-encoding steps; 16-min scan time] and a modified T2-weighted Hypercho sequence (3) (TE/TR, 42/10,000 ms; echo train length, 16,  $256 \times 256$  matrix size; 30 coronal slices;  $0.86 \times 0.86$ -mm in-plane resolution; 5-mm thickness; 1-mm gap; 2-min scan time), which were reviewed to rule out gross morphological abnormalities in the brain.

**Head Motion.** The framewise displacements from every time point,  $i$ , to the next were computed as follows:  $FD_i = |\Delta d_{ix}| + |\Delta d_{iy}| + |\Delta d_{iz}| + r|\Delta\alpha_i| + r|\Delta\beta_i| + r|\Delta\gamma_i|$ , from the translations ( $d_{ix}, d_{iy}, d_{iz}$ ) and rotations ( $\alpha_i, \beta_i, \gamma_i$ ) realignment parameters, and the root

mean square variance across voxels (DVARs) of the differences in percentage blood oxygen level-dependent intensity,  $I_i$ , between adjacent time points was computed as follows:

$DVARs_i = \sqrt{\langle [I_i - I_{i-1}]^2 \rangle}$  (brackets denote the average across imaging voxels). Note that angle rotations were converted to displacements using a radius  $r = 50$  mm, approximately the mean distance from the center of the Montreal Neurological Institute space to the cortex. Image time points with  $FD_i > 0.5$  mm and  $DVARs_i > 0.5\%$  were considered severely contaminated with motion artifacts and excluded from the time series (4).

In addition, a multilinear regression approach that used the time-varying realignment parameters (three translations and three rotations) was applied to minimize motion-related fluctuations in the MRI signals (5), and the global signal intensity was normalized across time points. Bandpass temporal filtering (0.01–0.10 Hz) was used to remove magnetic field drifts of the scanner and minimize physiologic noise of high-frequency components (5). Voxels with signal-to-noise (as a function of time)  $< 50$  were eliminated to minimize unwanted effects from susceptibility-related signal-loss artifacts.

**Anatomical and Network Labeling.** Anatomical labeling was based on the Automated Anatomical Labeling (AAL) atlas (6) and the population-average landmark- and surface-based (PALS) atlas of the cerebral cortex (7) provided in the installation package of the MRICron image viewer ([www.nitrc.org/projects/mricron](http://www.nitrc.org/projects/mricron)).

The AAL and PALS atlases were also used to identify voxels in subcortical regions and cerebellum. Voxels in the visual, default-mode (DMN), and dorsal attention (DAN) networks were identified as those functionally connected to the main hubs in cuneus (BA 18), ventral precuneus/posterior cingulum (BA 23/31; DMN hub), and inferior parietal cortex (BA 40; DAN hub) in a large sample of healthy subjects (8).

1. Tomasi D, Caparelli EC, Chang L, Ernst T (2005) fMRI-acoustic noise alters brain activation during working memory tasks. *Neuroimage* 27(2):377–386.
2. Lee JH, et al. (1995) High contrast and fast three-dimensional magnetic resonance imaging at high fields. *Magn Reson Med* 34(3):308–312.
3. Hennig J, Scheffler K (2001) Hyperchoes. *Magn Reson Med* 46(1):6–12.
4. Power JD, Barnes KA, Snyder AZ, Schlaggar BL, Petersen SE (2012) Spurious but systematic correlations in functional connectivity MRI networks arise from subject motion. *Neuroimage* 59(3):2142–2154.
5. Tomasi D, Volkow ND (2010) Functional connectivity density mapping. *Proc Natl Acad Sci USA* 107(21):9885–9890.

6. Tzourio-Mazoyer N, et al. (2002) Automated anatomical labeling of activations in SPM using a macroscopic anatomical parcellation of the MNI MRI single-subject brain. *Neuroimage* 15(1):273–289.
7. Van Essen DC, Glasser MF, Dierker DL, Harwell J, Coalson T (2012) Parcellations and hemispheric asymmetries of human cerebral cortex analyzed on surface-based atlases. *Cereb Cortex* 22(10):2241–2262.
8. Tomasi D, Volkow ND (2011) Association between functional connectivity hubs and brain networks. *Cereb Cortex* 21(9):2003–2013.





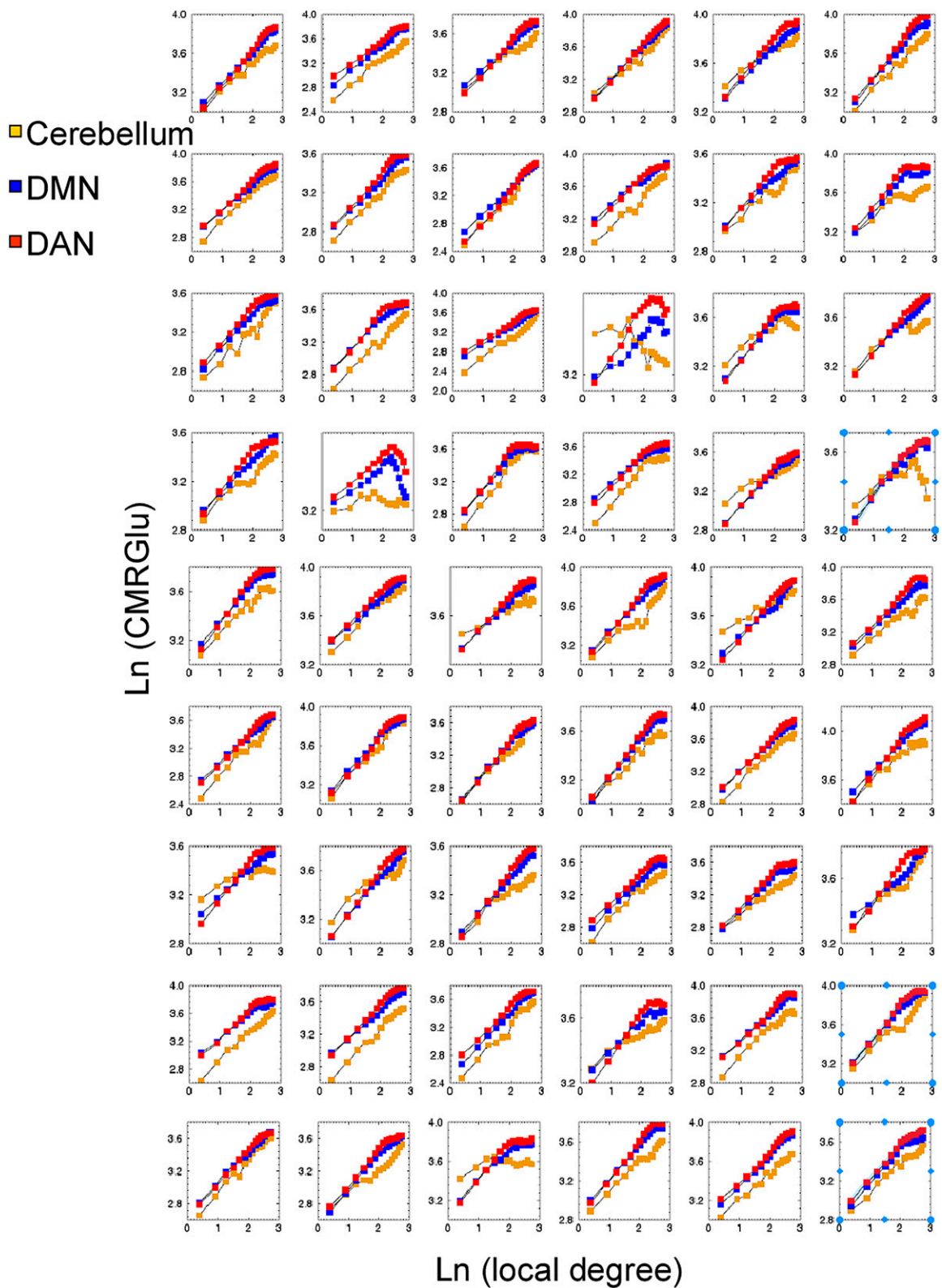


**Fig. S3.** Metabolic cost of the local degree centrality hubs for each subject and brain region. The logarithmic form of the power-scaling model fit the average values of CMRGlu and degree in  $\Delta k = 1$  bins for all subjects in the DMN and DAN, and cerebellum. Sample: 54 healthy subjects. A correlation threshold level  $R = 0.6$  was used to compute the degree centrality at 3-mm isotropic resolution.